Dynamic control of visible radiation by a liquid crystal filled Fabry-Pérot etalon

S. A. Jewell,[a] S. L. Cornford, and J. R. Sambles
Thin Film Photonics Group, School of Physics, University of Exeter, Stocker Road, Exeter, England EX4 4QL, United Kingdom

(Received 30 July 2007; accepted 17 September 2007; published online 15 November 2007)

A liquid crystal filled Fabry-Pérot etalon has been constructed to control the resonant transmission of electromagnetic radiation over the visible range of the spectrum. This has been achieved through the use of a 1.5 μm thick homogeneously aligned liquid crystal layer in the core of a silver-clad etalon structure. Applying an electric field across the core reorientates the liquid crystal director and changes the refractive index for incident light polarized parallel to the rubbing direction. By measuring the transmitted intensity as a function of wavelength for a variety of applied voltages shifts in the positions of the resonant transmission modes of up to 80 nm have been observed. In addition, these results have been compared to model data generated using a multilayer optics model to obtain the dispersion of the liquid crystal over the visible range of the electromagnetic spectrum.
 [DOI: 10.1063/1.2809448]

I. INTRODUCTION

The Fabry-Pérot etalon is a simple yet powerful technique for selecting the wavelength of transmission of electromagnetic radiation. The etalon requires a mirror-bound dielectric core with a thickness that is approximately a multiple of half the wavelength of the incident radiation within the dielectric. For a weakly absorbing dielectric core it also requires that for radiation over the visible range of the spectrum a cavity thickness of around a few microns or less is required, otherwise too much loss occurs. For radiation incident on the cavity at normal incidence the transmitted wavelengths, λ, are determined approximately by the expression $2nd=m\lambda$, where n is the refractive index of the core, d is the core thickness, and the integer m is the mode number. To alter the resonant wavelengths of the cavity it is therefore necessary to either change the thickness or the refractive index of the core. While adjusting the core thickness is often realized using piezodrivers with an air or vacuum filled cavity an alternative for a dielectric filled cavity is through control of the core refractive index. One method of achieving this is through the use of an aligned nematic liquid crystal in the core. As such materials are optically anisotropic, the refractive index of the material sensed by polarized light depends on the orientation of the average molecular direction (referred to as the director)[1] with respect to the incident polarization direction. Furthermore, if the mirrors of the etalon are metal layers these can be used as electrodes to apply an electric field across the core, allowing the director orientation (and hence the effective refractive index) to be controlled.

Previous studies of liquid crystal filled Fabry-Pérot etalons have generally concentrated on the near infrared region of the spectrum due to the significance of multiplexing such wavelengths for communications applications.[2–5] Such devices typically use a cavity thickness of the order of a few tens of microns and the transmitted intensities of high order modes are measured. In this study, we demonstrate how a liquid crystal filled Fabry-Pérot etalon of around a micron in thickness can be used as a highly effective method for controlling the transmission of radiation in the visible range of the electromagnetic spectrum. Overcoming the significant challenges of constructing an ultrathin cavity while maintaining the electrical isolation of the cavity walls over the active area allows the discrete modes of the cavity to be tuned. Furthermore, through analyzing such an optical system and comparing it to a multilayer optics model, the optical dispersion of the liquid crystal material can be determined over the visible range of the electromagnetic spectrum. This is in contrast to more established refractive index measurement techniques which tend to be restricted to single wavelengths.[6–8]

II. EXPERIMENTAL

A Fabry-Pérot etalon was constructed from two identical silica substrates, each of which had a 20 nm thick silver stripe of width 4 mm evaporated onto one surface to act as both a partially reflecting mirror and an electrode. On top of this layer a 15 nm layer of SiO_x was evaporated at a 60° angle of incidence to produce a homogeneously aligning surface with the evaporation direction parallel to one silver stripe and perpendicular to the other. The cell was then assembled using glass beads of nominal thickness 1 μm in UV curing glue as spacers along the edge of the cavity, with the two silver stripes crossed. The purpose of this was to produce a minimal overlap region for the electrodes to reduce the risk of the cell shorting (Fig. 1 inset). The uniaxial liquid crystal E7 (BL001, Merck KGa) was introduced into the cell at room temperature to produce a homogeneously aligned cell and wires were attached to the exposed regions of the silver stripes. The cell was mounted in the monochromator setup shown in Fig. 1 with the liquid crystal director oriented along the y-axis and the cell face at normal incidence to the beam. For incident light polarized either parallel to (y polarized) or perpendicular to (x polarized) the rubbing direction

[a]Electronic mail: s.a.jewell@exeter.ac.uk

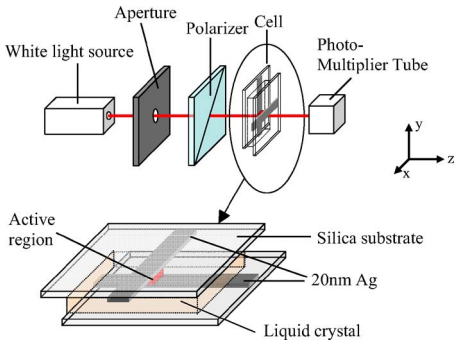

FIG. 1. (Color online) Schematic diagram of the layout of the experiment and the cell structure used.

of the cell the transmitted intensity was recorded as a function of wavelength over the range of 440–825 nm in 1 nm steps. This was then repeated with various 10 kHz sinusoidal ac voltages applied across the cell for both polarizations, up to a maximum voltage of 20 V (peak to peak). The data was then normalized to a spectrum from a nonperturbed monochromator beam to allow the absolute transmission versus wavelength for each set of data to be obtained.

III. RESULTS AND DISCUSSION

The normalized transmitted intensity measured as a function of wavelength and peak-to-peak voltage for *x*- and *y*-polarized light is shown in Fig. 2. It was noted that due to the low resistance of the thin liquid crystal layer (arising from the relatively low resistivity of E7) the voltage across the cell was noticeably lower than the applied voltage. The resistance of the sample was measured by connecting a multimeter across the cell. The recorded resistance varied with the director orientation, ranging from $210\pm5\ \Omega$ at 0 V to $110\pm5\ \Omega$ when fully homeotropically aligned. This resulted in a nonlinear relationship between the applied and measured peak-to-peak voltages, with an applied voltage of 20 V_{pp} resulting in potential difference of 13.6 V_{pp} being measured across the cell and from here in the voltages referred to are the measured voltages across the cell.

It can clearly be seen that the *y*-polarized light is highly sensitive to the applied voltage (and hence the tilt of the director in the bulk of the cell) due to the polarization of the light in this case being parallel to the rubbing direction. For this data set no change in the optical response of the cell occurs before the Freedericksz threshold[1] at a potential difference of around 1.8 V_{pp}. Beyond this threshold the positions of the modes steadily shift down in wavelength as the voltage increases (and hence the effective refractive index in the cavity decreases) with the cell fully switched into the homeotropic state at an applied voltage of 13.6 V_{pp}. The amount that the resonances shift by varies from $92(\pm1)$ nm for the $n=6$ mode to $55(\pm2)$ nm for the $n=10$ mode. In contrast, the position of the modes in the data set collected for the *x*-polarized light shows a small yet measurable shift downwards in frequency as the voltage is increased, again suggesting a slight change in the optical properties of the cavity, as discussed later.

Figure 3 shows comparisons between various data sets collected for *x*- and *y*-polarized light at 0 and 13.6 V. Figure 3(a) is for the *x*- and *y*-polarized light collected at 0 V and the modes present in these two data sets initially appear to bear close resemblance to each other. However, as seen by the movement of the mode in the gray-scale plot shown in Fig. 2 this is not the case, and, in fact, the modes that appear to be closely overlapping for *y*- and *x*-polarized data are actually of different orders. Figure 3(b) illustrates the effect on the transmission through the cell when a large voltage is applied to induce homeotropic alignment. In this case both the *y*- and *x*-polarized data sets overlie each other extremely close. This suggests that both polarizations of light are experiencing the same refractive index within the cell (n_o), indicating that the cell has good homeotropic alignment. It is also interesting to note in Fig. 3(b) that the 13.6 V *x*-polarized data are almost uniformly shifted down in wavelength from the 0 V *x*-polarized data by around 8 nm. This indicates that at 0 V the *x*-polarized light experiences an optical path length which is marginally lower than at 13.6 V, as discussed later.

Figure 4 shows the positions of the resonant frequencies for the *y*-polarized data at 0 and 13.6 V plotted against mode

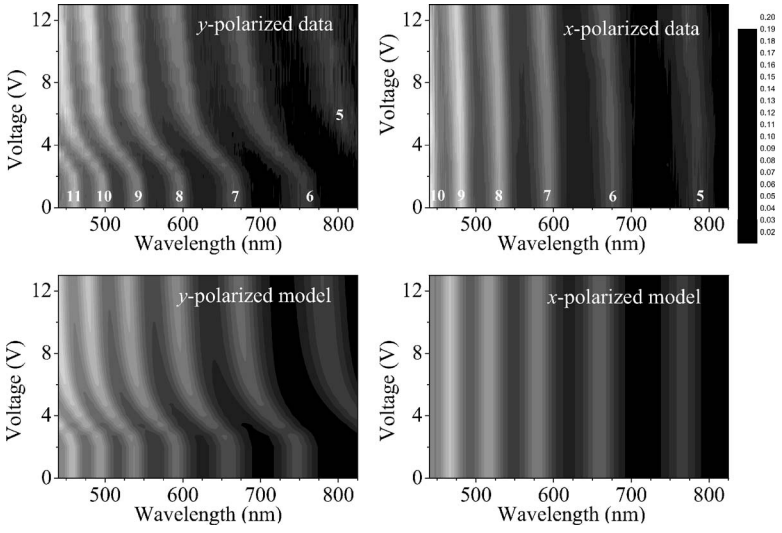

FIG. 2. Gray scale plot of the data for light polarized (a) parallel to and (b) perpendicular to the director *n* and [(c) and (d)] the results of modeling the transmitted light intensity for the same polarizations. The labels on the plots indicate the specific mode numbers.

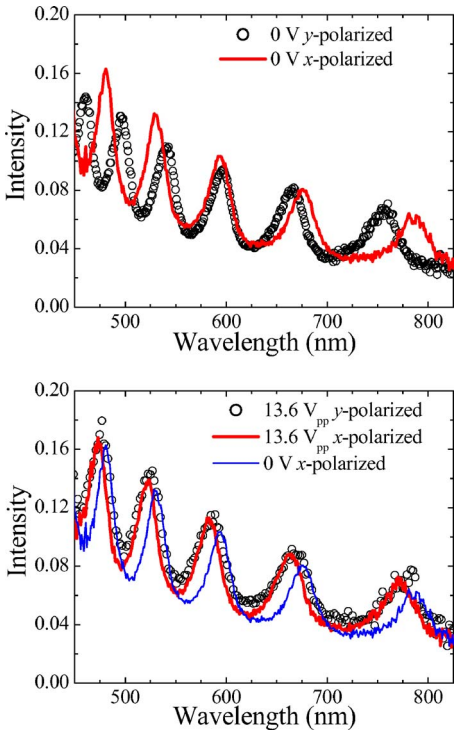

FIG. 3. (Color online) Examples of transmitted intensity vs wavelength data collected for (a) no applied voltage and (b) 20 V applied.

number and the result of fitting a linear regression to the data. As expected, to a first approximation the modes appear to be regularly spaced in frequency with the 13.6 V data showing a particularly good linear trend. However, a possible slight deviation may occur due to the dispersion of the liquid crystal, as discussed later.

To obtain a more thorough understanding of the optical response of the Fabry-Pérot etalon optical intensity versus wavelength data for each of the applied voltages were fitted to simultaneously using a multilayer optics modeling code based on a 4×4 Berreman matrix method,[9] which accounts for both anisotropy and multiple beam interference in planar structures which vary in one dimension (1D). The code used the elastic and dielectric constants of E7 to model the director profile of the cell at each voltage which was then used to calculate the transmitted intensity. The splay and bend elastic coefficients (k_1 and k_3) and dielectric permittivities ($\varepsilon_{\parallel}$ and $\varepsilon_{\perp}$) of the liquid crystal along with the thickness of the liquid

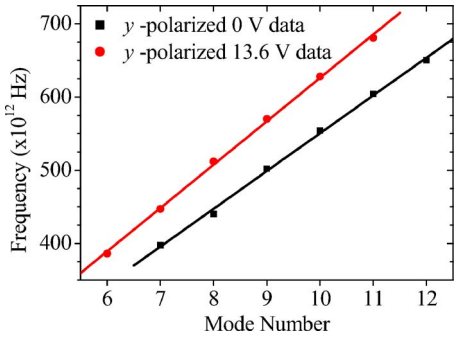

FIG. 4. (Color online) Demonstration of frequency vs mode number for homeotropic and homogeneous alignments in the cell.

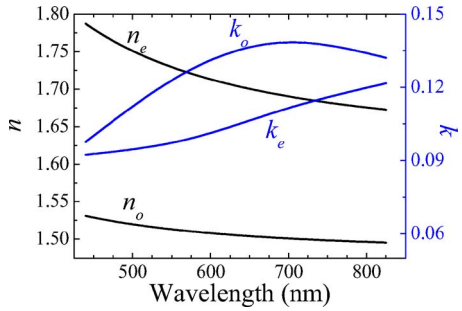

FIG. 5. (Color online) Modeled dispersion of n and k values of E7 at visible frequencies.

crystal and silver layers were used as fitting parameters. Crucially, the fitting routine also included the dispersion of the real and imaginary components of the ordinary and extraordinary optical permittivities of the E7 (modeled as a parabola and a cubic spline, respectively), and used published values for the dispersion of the silver layers.[10] The resulting model data for the transmitted intensity as a function of voltage and wavelength for x- and y-polarizations are shown in Figs. 2(c) and 2(d) respectively. The physical liquid crystal constants produced were $k_1=11.7$ pN, $k_3/k_1=1.675$, and $\Delta\varepsilon=13.0$ (±0.1) and the refractive indices were modeled as $n_o=1.456\ (\pm0.001)+[9.7(\pm0.5)\times10^3]/\lambda^2$ and $n_e=1.618\ (\pm0.001)+[30.9(\pm0.4)\times10^3/\lambda^2]$ where λ is the wavelength (in nanometers) with a cubic spline being used to model the imaginary component of the refractive indices, k_o and k_e, as shown in Fig. 5. The thickness of the liquid crystal layer was determined as 1.50 μm and the silver layers were both 16.9 nm with the azimuth of the director set at a 0.4° angle from the y-axis and at normal incidence to the incident beam. The values for n show good agreement with values previously published for E7.[11] However, the values for k appear to be rather higher than expected; this may be due to other sources of loss in the system, such as the 1.5 mm thick silica substrates which had not been allowed for in the model.

Good agreement was found between the initial and final positions of the modes in the experimental and model data for the two polarization states and the voltage of the Freedericksz transition in the y-polarized data. When the model and measured data for the x-polarized case is compared the slight shift in mode position with voltage observed experimentally is not apparent in the model data. Closer examination of the x-polarized data shows that the data show no noticeable shift until around 8 V is applied to the cell, which is significantly higher than the Freedericksz threshold of the system. This suggests that the shift is not simply due to a small azimuthal offset of the cell substrates or a slightly off-set azimuth; this has been confirmed through the modeling as a significant change in azimuth would be required to produce such a change. It is likely that this small yet measurable change in mode position arises from an attraction between the two electrodes due to the high electric field applied. A change in thickness of ~2%, corresponding to a radius of curvature of the 2 mm thick silica substrate of around 1.8×10^3 m is sufficient to produce the observed mode shift and using a simple

model where the elastic energy of the system is proportional to the square of the thickness change suggests that such a deformation is plausible.

Both sets of data may also be affected by other sources of experimental error, such as edge effects in the vicinity of the crossed electrode producing a nonuniform reorientation in the switching region of the cell. Extending the model used in this study from 1D to two-dimensional variations would allow the significance of such an effect on the alignment in the active region to be assessed. Beam clipping at the crossed electrode region and a variation in the cell thickness across the active region could also have an effect despite steps being taken to minimize this.

IV. CONCLUSIONS

It has been shown that a Fabry-Pérot cavity with a core thickness of the order of 1 μm and filled with a homogeneously aligned nematic liquid crystal can be used to control the resonantly transmitted wavelengths of visible radiation. By using an applied electric field to control the orientation of the liquid crystal director shifts in the mode positions of up to 80 nm can be achieved. Comparing the transmitted intensity versus wavelength as a function of voltage to model data generated using a multilayer optics modeling code also allows the structure to be used to determine the refractive index of the liquid crystal material over the visible spectrum. Through the optimization of such a structure through the use of a thinner core (while maintaining the electrical isolation of the cavity walls) and an optimized liquid crystal material the dynamically tunable Fabry-Pérot etalon may provide a route to producing efficient color displays by replacing the current need for color filters in portable displays.

ACKNOWLEDGMENTS

The authors would like to acknowledge financial support for this work from the Engineering and Physical Sciences Research Council in the UK.

[1] P. G. De Gennes, *The Physics Of Liquid Crystals* (Clarendon, Oxford, 1974).
[2] J.-H. Lee, H.-R. Kim, and S.-D. Lee, Appl. Phys. Lett. **75**, 859 (1999).
[3] J. S. Patel and S.-D. Lee, Appl. Phys. Lett. **58**, 2491 (1991).
[4] H. R. Kim, E. J. Jang, J. Im, and S. D. Lee, Jpn. J. Appl. Phys., Part 1 **35**, 2156 (1995).
[5] Y. H. Huang, T. X. Wu, and S. T. Wu, J. Appl. Phys. **93**, 2490 (2003).
[6] S. A. Jewell, J. R. Sambles, J. W. Goodby, A. W. Hall, and S. J. Cowling, J. Appl. Phys. **95**, 2246 (2004).
[7] S. A. Jewell and J. R. Sambles, Opt. Express **13**, 2627 (2005).
[8] F. Z. Yang, S. A. Jewell, L. Z. Ruan, and J. R. Sambles, J. Opt. Soc. Am. B **24**, 527 (2007).
[9] D. Y. K. Ko and J. R. Sambles, J. Opt. Soc. Am. A **5**, 1863 (1988).
[10] E. D. Palik, *Handbook of Optical Constants of Solids* (Academic, New York, 1985).
[11] C. V. Brown, E. E. Kriezis, and S. J. Elston, J. Appl. Phys. **91**, 3495 (2002).